

Adaptive thermogenesis in brown adipose tissue involves activation of pannexin-1 channels



Subramanian Senthivinayagam¹, Vlad Serbulea¹, Clint M. Upchurch¹, Renata Polanowska-Grabowska¹, Suresh K. Mendu¹, Srabani Sahu¹, Prathiba Jayaguru³, Kevin W. Aylor⁴, Mahendra D. Chordia⁵, Limor Steinberg¹, Nathaniel Oberholtzer¹, Seichii Uchiyama⁶, Noriko Inada⁷, Ulrike M. Lorenz⁹, Thurl E. Harris¹, Susanna R. Keller⁴, Akshaya K. Meher¹, Alexandra Kadl³, Bimal N. Desai¹, Bijoy K. Kundu^{5,8}, Norbert Leitinger^{1,2,*}

ABSTRACT

Objective: Brown adipose tissue (BAT) is specialized in thermogenesis. The conversion of energy into heat in brown adipocytes proceeds via stimulation of β -adrenergic receptor (β AR)-dependent signaling and activation of mitochondrial uncoupling protein 1 (UCP1). We have previously demonstrated a functional role for pannexin-1 (Panx1) channels in white adipose tissue; however, it is not known whether Panx1 channels play a role in the regulation of brown adipocyte function. Here, we tested the hypothesis that Panx1 channels are involved in brown adipocyte activation and thermogenesis.

Methods: In an immortalized brown pre-adipocytes cell line, Panx1 currents were measured using patch-clamp electrophysiology. Flow cytometry was used for assessment of dye uptake and luminescence assays for adenosine triphosphate (ATP) release, and cellular temperature measurement was performed using a ratiometric fluorescence thermometer. We used RNA interference and expression plasmids to manipulate expression of wild-type and mutant Panx1. We used previously described adipocyte-specific Panx1 knockout mice (Panx1^{Adip-/-}) and generated brown adipocyte-specific Panx1 knockout mice (Panx1^{BAT-/-}) to study pharmacological or cold-induced thermogenesis. Glucose uptake into brown adipose tissue was quantified by positron emission tomography (PET) analysis of ¹⁸F-fluorodeoxyglucose (¹⁸F-FDG) content. BAT temperature was measured using an implantable telemetric temperature probe.

Results: In brown adipocytes, Panx1 channel activity was induced either by apoptosis-dependent caspase activation or by β 3AR stimulation via a novel mechanism that involves G $\beta\gamma$ subunit binding to Panx1. Inactivation of Panx1 channels in cultured brown adipocytes resulted in inhibition of β 3AR-induced lipolysis, UCP-1 expression, and cellular thermogenesis. In mice, adiponectin-Cre-dependent genetic deletion of Panx1 in all adipose tissue depots resulted in defective β 3AR agonist- or cold-induced thermogenesis in BAT and suppressed beigeing of white adipose tissue. UCP1-Cre-dependent Panx1 deletion specifically in brown adipocytes reduced the capacity for adaptive thermogenesis without affecting beigeing of white adipose tissue and aggravated diet-induced obesity and insulin resistance.

Conclusions: These data demonstrate that G $\beta\gamma$ -dependent Panx1 channel activation is involved in β 3AR-induced thermogenic regulation in brown adipocytes. Identification of Panx1 channels in BAT as novel thermo-regulatory elements downstream of β 3AR activation may have therapeutic implications.

© 2020 The Authors. Published by Elsevier GmbH. This is an open access article under the CC BY-NC-ND license (<http://creativecommons.org/licenses/by-nc-nd/4.0/>).

Keywords adipocyte; brown adipose tissue; Thermogenesis; Pannexin channels

1. INTRODUCTION

Brown adipose tissue (BAT) regulates the adaptation to cold as well as diet-induced thermogenesis [1,2]. Brown adipocytes are highly specialized cells that dissipate energy in the form of heat [3], a process that in mice is typically induced via activation of β 3-

adrenergic receptors (β 3AR) [4–6]. The predominant mediator of thermogenesis is mitochondrial uncoupling protein 1 (UCP1) [7–10], which is functionally inhibited by nucleotides adenosine triphosphate (ATP) or adenosine diphosphate (ADP) [11–14] and activated by fatty acids generated via lipolysis, or as recently shown, by lipolysis-independent mechanisms [15,16]. However, knowledge about

¹Department of Pharmacology, University of Virginia School of Medicine, Charlottesville, VA, 22908, USA ²Robert M Berne Cardiovascular Research Center, University of Virginia, Charlottesville, VA, 22908, USA ³Division of Pulmonary and Critical Care Medicine, Department of Medicine, University of Virginia, Charlottesville, VA, 22908, USA ⁴Division of Endocrinology and Metabolism, Department of Medicine, University of Virginia, Charlottesville, VA, 22908, USA ⁵Department of Radiology and Medical Imaging, University of Virginia School of Medicine, Charlottesville, VA, 22908, USA ⁶Graduate School of Pharmaceutical Sciences, The University of Tokyo, Tokyo, Japan ⁷Graduate School of Life and Environmental Sciences, Osaka Prefecture University, Osaka, Japan ⁸Department of Biomedical Engineering, University of Virginia School of Medicine, Charlottesville, VA, 22908, USA ⁹Department of Microbiology, Immunology and Cancer Biology, Center for Cell Clearance, the Beirne B. Carter Center for Immunology Research, USA

*Corresponding author. Department of Pharmacology, University of Virginia, 1340 Jefferson Park Ave, Charlottesville, VA, 22911, USA. E-mail: nl2q@virginia.edu (N. Leitinger).

Received April 29, 2020 • Revision received November 6, 2020 • Accepted November 21, 2020 • Available online 25 November 2020

<https://doi.org/10.1016/j.molmet.2020.101130>

additional mechanisms that control adrenergic signaling-induced thermogenesis is limited.

Pannexin-1 (Panx1) is a membrane channel that is structurally similar to connexins but does not form gap-junctions [17]. Activation of Panx1 that leads to channel opening proceeds via a variety of mechanisms [18,19], including reversible α 1-adrenergic stimulation [20,21] and irreversible caspase-mediated cleavage of the C-terminal portion of Panx1, which occurs during apoptosis [22,23]. A recent high-resolution single particle structural analysis of human Panx1 using cryo-electron microscopy revealed human Panx1 channels to be heptamers with a wide main pore and side tunnels and identified the 7 W74 residues on the extracellular domain as the binding site for carbenoxolone, a widely used pharmacological inhibitor of Panx1 [24]. Many of the biological effects mediated by Panx1 have been attributed to the release of ATP, which in turn regulates autocrine and paracrine purinergic signaling. ATP released from apoptotic cells via Panx1 serves as a “find-me” signal for phagocytes [22], facilitating efferocytosis. Panx1 channel function is also regulated by posttranslational modification, such as phosphorylation and S-nitrosylation [25–27]. Pharmacological inhibitors of Panx1 include carbenoxolone, probenecid, mefloquine, the food dye FD&C Blue No. 1, trovafloxacin, and spironolactone [28–31].

We and others have previously demonstrated a functional role for Panx1 channels in white adipose tissue [32–34]. We found that Panx1 channel function in white adipocytes is required for full activation of insulin-induced glucose uptake, and adipocyte-specific Panx1 knock out mice exhibited exacerbated insulin-resistance under a high-calorie diet [32]. However, whether Panx1 channels play a role in the regulation of brown adipocyte function is not known. Here, we discover a novel mechanism by which Panx1 channels are activated by β 3-adrenergic stimulation to control the β AR-induced thermogenic response in brown adipocytes.

2. MATERIALS AND METHODS

2.1. Reagents

CL316243, forskolin, ^8Br -cAMP, ARL 67156 trisodium salt, and suramin were procured from Tocris (Minneapolis, MN). Carbenoxolone, trovofloxacin, and spironolactone were from Sigma Aldrich (St. Louis, MO). Silencer select siRNAs against mouse Panx1 (assay ID-s79985) or mouse G β subunits (GNB1 – assay ID –ss66813; GNB2 – assay ID –ss66816; GNB3 – assay ID –ss66822; GNB4 – assay ID –n420113) and silencer select negative control-2 siRNA (4390846) were purchased from ThermoFisher Scientific (Middletown, VA). Antibodies used in the study were as follows: mouse monoclonal anti-Panx1 (Clone 720505, #MAB7097) was from R&D Systems (Minneapolis, MN); rabbit-polyclonal anti-UCP1 (#U6382) was from Sigma–Aldrich (St. Louis, MO); mouse monoclonal OXPHOS antibody cocktail (#MS604) was from Mitosciences (Eugene, OR); rabbit monoclonal anti-Panx1 antibody (Clone D9M1C, #91137), anti-PKC phosphorylation antibody sampler kit (#9921) and rabbit monoclonal anti-vinculin (Clone E1E9 V, #13901) were from Cell Signaling (Danver, MA). Cellular glucose uptake was measured using a glucose uptake-Glo assay kit (#J1341, Promega, Madison, WI).

2.2. Animals

Adipocyte-specific Panx1 knockout mice (Panx1^{Adip}^{-/-}) used in the study have been previously described [32]. Brown adipocyte-specific Panx1 knock out mice (Panx1^{BAT}^{-/-}) were generated by breeding Panx1^{fl/fl} mice with transgenic mice expressing Cre under the control of the UCP1 promoter (Jackson Laboratories, stock # 024670). Mice

were maintained in a pathogen-free animal facility under 12-hour light/dark cycles and had access to food and water *ad libitum*. For cold exposure, mice were housed individually at 4 °C for 3 days. For β 3-adrenergic stimulation, mice were given an intraperitoneal injection of CL316243 (1 mg/kg) every day for 6 days. All experiments were approved by the Institutional Animal Care and Use Committee (IACUC) of the University of Virginia.

2.3. PET

Glucose uptake into BAT was quantified by PET analysis of ^{18}F -fluorodeoxyglucose (^{18}F -FDG) uptake. Procurement of FDG was from PETNET Solutions, Inc. of Charlottesville, VA. The mice were fasted overnight before PET/CT studies. On the day of imaging, mice were given an intraperitoneal injection of CL316243 (1 mg/kg b. wt). Thirty minutes after injection of CL316243, ^{18}F -FDG (100 μCi) was administered through tail vein injection under isoflurane anesthesia. Imaging was performed 90 min later under the same anesthesia while maintaining body temperature using a Focus F-120 small-animal microPET scanner (Siemens Medical Solutions, Inc.) following a previously published protocol [33]. Each PET acquisition was performed for 10 min. PET images were reconstructed from raw data with the OSEM3D/MAP algorithm (zoom factor, 2.164) using microPET Manager (version 2.4.1.1, Siemens). The reconstructed pixel size was 0.28 \times 0.28 \times 0.79 mm on a 128 \times 128 \times 95 image matrix. All PET images were normalized to decay correction but not for attenuation. Each image analysis was performed using ASIPRO software (Siemens) for presentation. The final PET images were used for quantitative estimates of the accumulation of ^{18}F -FDG in the regions of interest (ROI) of BAT, and the maximum standardized uptake values (SUV) were calculated from the maximum pixel value in the image slice.

2.4. Glucose and insulin tolerance tests

Mice were fasted for 6 h before performing glucose or insulin tolerance tests. For glucose tolerance test, mice received an intraperitoneal injection of glucose (1 mg/g b. wt.), and blood glucose was measured before and at 0, 15, 30, 60, 90, and 120 min after injection. For insulin tolerance test, mice received an intraperitoneal injection of insulin (0.5 U/kg b. wt.), and blood glucose was measured before and at 0, 15, 30, 45, and 60 min of injection.

2.5. Measurement of BAT temperature

BAT temperature was measured using an implantable telemetric temperature probe (Bio Medic Data Systems, Inc., Seaford, DE). A day before cold exposure, mice were anesthetized and the telemetric probe supplied in a sterile disposable needle unit was injected subcutaneously in the interscapular region. After 24 h, mice were placed in the cold. Temperature readings were taken by placing a hand-held digital receiver (Model #IPTT, BMDS) above the interscapular region of the free-moving mice.

2.6. Adipocyte histology and immunohistochemistry

Five-microgram sections of formalin fixed brown adipose tissue (BAT) and inguinal subcutaneous white adipose tissue (scWAT) were stained with hematoxylin and eosin. Adipocyte size distribution in brown adipose tissue was measured using ImageJ with the “Adipocyte tool” macro (<http://dev.mri.cnrs.fr/projects/imagej-macros>). Analysis was performed by a person blinded to the experimental paradigms.

2.7. Cell culture

An immortalized brown pre-adipocytes cell line (iBAC) was maintained in Dulbecco’s modified Eagle’s medium (DMEM) containing 20% fetal

bovine serum (FBS). Cells were differentiated into mature adipocytes as described [35] and used for experimentation after 6 days. 293 T cells (American Type Culture Collection, ATCC) were maintained in 10% DMEM with antibiotics. Cell lines used in the study were negative for mycoplasma contamination. Cells were pretreated with Panx1 inhibitors (carbenoxolone - 50 μ M; probenecid - 1 mM; trovafloxacin - 50 μ M; spironolactone - 50 μ M) for 60 min and then treated with CL316243 (100 nM for iBACs and 200 nM for 293T) for indicated time periods.

2.8. Measurement of Panx1 currents

Panx1 currents in iBACs were measured using patch-clamp electrophysiology as described previously [23]. Cells were exposed to 200 mJ/cm² of ultraviolet (UV)-irradiation and 2 h later, whole-cell recordings at room temperature were made using Axopatch 200 B amplifier (Molecular Devices) in a bath solution composed of 140 mM of NaCl, 3 mM of KCl, 2 mM of MgCl₂, 2 mM of CaCl₂, 10 mM of HEPES, and 10 mM of glucose (pH 7.3). Borosilicate glass patch pipettes (3–5 M Ω) were filled with an internal solution containing 30 mM of tetraethylammonium chloride, 100 mM of CsMeSO₄, 4 mM of NaCl, 1 mM of MgCl₂, 0.5 mM of CaCl₂, 10 mM of HEPES, 10 mM of EGTA, 3 mM of ATP-Mg, and 0.3 mM of GTP-Tris (pH 7.3). Ramp voltage commands were applied by using pCLAMP software and Digidata1322 A digitizer (Molecular Devices, San Jose, CA). Basal Panx1 current was recorded, and then the Panx1 inhibitor carbenoxolone (CBX, 50 μ M) was applied to the bath solution.

2.9. Caspase-3/7 assay

iBACs were plated in 24-well plates at a density of 5×10^5 cells/well in differentiation media. The next day, fresh serum free media was added and kept at 37 °C cell culture incubator for 2 hrs. Next, cells were exposed to 200 mJ/cm² UV-irradiation and caspase activity was measured 1 h after exposure using the caspase Glo 3/7 assay kit (#G8091, Promega, Madison, WI).

2.10. Extracellular ATP measurement

ATP concentration in the cell culture media was measured using CellTiter-Glo Luminescent cell viability assay kit (#G7571, Promega, Madison, WI). Briefly, iBACs (5×10^5 cells/well) were plated in 24-well plates in differentiation media. The next day, 500 μ l of fresh serum-free media was added and incubated at 37 °C for 3 h. Then, 50 μ l of media was removed and 50 μ l of serum-free media containing 10x Panx1 inhibitors were added for an additional 60 minutes. At the end of the incubation time, 20 μ l of media was removed and 20 μ l of fresh serum-free media containing 20x CL316243 was added to the media and incubated further. After 30 min, 25–30 μ l of media was collected from each well with utmost care not to touch the cells at the bottom of the wells. The media was then centrifuged at 3,000 rpm for 5 min, and the ATP concentration in the supernatant was measured immediately.

2.11. Plasmids and transfection

Untagged-Panx1 and GFP-tagged Panx1 plasmids have been described previously [36]. Panx1 mutant lacking putative G β γ binding site (Panx1- Δ G β γ) was made with the following primers (forward-CAATCTTTGAACTCCAGCTCTCCCTTGGTCT; reverse-AGACCAAGGGA GAGGACGTGG AGTTCAAAGATTTG) using a quick-change site directed mutagenesis kit (Agilent Technologies, Santa Clara CA). cDNA clone for mouse myc-DDK-adrenergic receptor beta-3 (ADRB3) (MR225687) was purchased from Origene (Rockville, MD). To generate mCherry-tagged-mADRB3, mADRB3 was polymerase chain reaction (PCR) amplified with SpeI-NotI restriction sites from the

Origene clone without myc-DDK and cloned into pcDNA3.1 E5-spGFP1-10-TevS-K5 T2A mCherry (pTLT848). cDNA clones for the c-terminal region of β -adrenergic receptor kinase (β -ARK-CT) and G α s (transducin) were described previously [37]. Cells were transfected with the plasmids using Lipofectamine 3000 reagent (ThermoFisher Scientific, Middletown, VA) according to the manufacturer's protocol.

2.12. Flow cytometric analysis of To-Pro-3 uptake

293T cells (American Type Culture Collection, ATCC) in 12-well plates were transfected with GFP, GFP-Panx1, or GFP-Panx- Δ G β γ mutant and mCherry-T2A-mADRB3 plasmids. Forty-eight hours later, cells were treated with 200 nM of CL316243 for 30 min in the presence of 1 μ M of To-Pro-3 (ThermoFisher Scientific, Middletown, VA). Cells were gated on GFP⁺, mCherry⁺ or GFP⁺mCherry⁺, and the percentage of cells positive for To-Pro-3 was measured before and after CL316243 treatment. Flow cytometry assay and data analysis were performed by a person blinded to the experimental paradigms.

2.13. Co-immunoprecipitation and immunoblotting

Tissues and cells were lysed in 1x radioimmunoprecipitation assay (RIPA) buffer (Millipore, Burlington, MA) containing protease inhibitors cocktail and phosphatase inhibitors 2 and 3 (Sigma—Aldrich, St. Louis, MO), and lysates were prepared by centrifugation at 13,000 rpm for 15 min at 4 °C. For immunoprecipitation, protein concentration was measured using protein assay BCA reagent kit (ThermoFisher Scientific, Middletown, VA). For immunoprecipitation, antibodies (2 μ g) were premixed with 30 μ l of Protein G beads (Sigma—Aldrich, St. Louis, MO) for 3–4 h at 4 °C and washed 3 times with lysis buffer. Lysates containing 100 μ g of protein were added to the antibody/bead premix, incubated overnight at 4 °C and washed 3 times with lysis buffer. For immunoblotting, lysate or immunoprecipitated samples were separated on 10% polyacrylamide gel electrophoresis (PAGE) and transferred to nitrocellulose membrane (BioRad, Hercules, CA) incubated overnight with primary antibodies and developed using Licor Odyssey Infrared system (Licor, Lincoln, NE). Densitometric analysis of the blots was performed using ImageJ.

2.14. Quantitative real-time PCR

Total RNA from cells and tissues were isolated using RNeasy kit (Qiagen) and reverse transcribed using an iScript cDNA synthesis kit (Bio-Rad, Hercules, CA). QRT-PCR was performed using Sensimix-SYBR Fluorescein kit (Bioline, Memphis, TN), and data were normalized to β 2-microglobulin (β 2m). PCR primers were obtained from mouse Primer Depot and verified using NCBI-Primer Blast. The primer sequences are listed in Table S2.

2.15. RNA interference

Adherent iBACs in 24-well plates were transfected with 50 nM of negative control siRNA or siRNAs against Panx1 or G β subunits using siPORTamine transfection reagent (ThermoFisher Scientific, Middletown, VA) following the manufacturer's protocol. Experiments were performed 48 h after transfection with siRNAs.

2.16. Single-cell thermometry

Cellular temperature measurement was performed using a ratiometric fluorescence thermometer [38]. The fluorescence thermometer consists of 4 units: (i) a cationic APTMA (3-acrylamidopropyl)trimethylammonium unit that enables the spontaneous entry into the cells, (ii) a thermosensitive NNPAM (N-n-propylacrylamide) unit that assumes an extended structure at low temperatures but attains a reduced globular structure at high temperatures, (iii) a fluorescent DBThD-AA

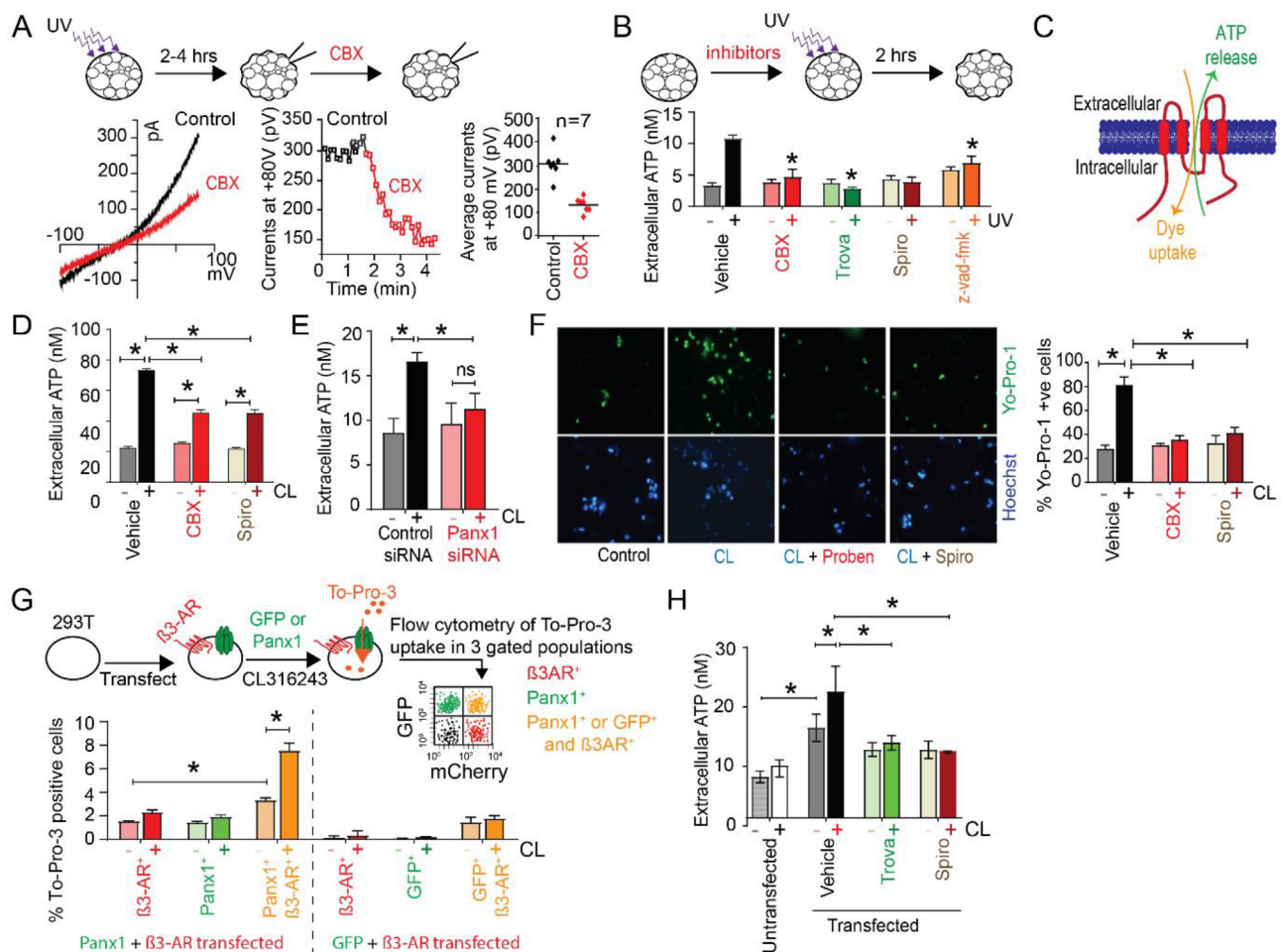


Figure 1: Apoptosis or β 3-adrenergic stimulation activate Panx1 channels in brown adipocytes. **A**, Immortalized pre-adipocytes differentiated into mature adipocytes (iBACs) were exposed to 200 mJ/cm² UV-irradiation and carbenoxolone-sensitive Panx1 currents were measured by whole-cell patch-clamp analysis. Representative current–voltage (I–V) graph (left), patch-clamp recording at +80 mV (middle), and average current densities (right) are shown. **B**, Panx1-dependent ATP release from iBACs subjected to UV-irradiation as in **A**, in the presence or absence of Panx1 inhibitors, or a pan-caspase inhibitor (50 μ M). **C**, Schematic showing activated Panx1 channel that allows for the release of ATP and the entry of fluorescent dyes. **D**, ATP release in iBACs treated with 100 nM of CL216343 for 30 min in the presence or absence of Panx1 inhibitors (50 μ M). **E**, ATP release from iBACs transfected with 50 nM control or Panx1 siRNA for 48 h and then treated with 100 nM of CL216343 for 30 min. **F**, Representative images and quantification of β 3-agonist induced Yo-Pro-1 dye uptake in iBACs, which were pre-treated with Panx1 inhibitors (50 μ M of spirinolactone or 1 mM of probenecid) and then treated with 100 nM of CL316243 for 30 min. **G**, Flow cytometric analysis of To-Pro-3 uptake in 293T cells transfected with GFP-Panx1 and mCherry- β 3AR (left), or GFP control and mCherry- β 3AR (right). **H**, ATP release from 293T cells transfected with Panx1 and β 3AR as in **G**. Forty-eight hours after transfection, cells were treated with 200 nM of CL316243 for 30 min. Statistical significance was calculated using Two-way ANOVA with Tukey's post-hoc test. * indicates $p < 0.05$. Error bars, s. e.m. Experiments were performed with a minimum of 3 replicates and repeated at least twice. CBX, carbenoxolone; Trova, trovafloxacin; Spiro, spirinolactone; Proben, probenecid.

(N-(2-[7-(N,N-dimethylaminosulfonyl)-2,1,3-benzothiadiazol-4-yl]- (methyl)amino-ethyl)-N-methylacrylamide) unit that senses the structural change in the NNPAM units and produces a temperature-dependent fluorescence and (iv) a fluorescent BODIPY-AA(8-(4-acrylamidophenyl)-4,4-difluoro-1,3,5,7-tetramethyl-4-bora-3a, 4a-diaza-s-indacene) unit that emits constant fluorescence as a reference signal. The fluorescent ratio at two different wavelengths is used as a temperature-dependent measurable parameter. iBACs plated on coverslips were pre-treated with indicated Panx1 inhibitors, then treated with 100 nM of CL316243 for 2 h. Subsequently, 0.05% of the probe in 5% glucose was added to the cells, incubated at 25 °C for 10 min, and rinsed with phosphate-buffered saline (PBS) before adding DMEM. The coverslip was then placed under a confocal microscope with a 100x lens. Single cells were excited at 473 nm and emission spectra collected at different wavelengths. Cellular temperature was

determined using a ratio of fluorescence intensity (FI) 575 nm:513 nm. Data analysis was performed by an individual blinded to experimental treatments.

3. RESULTS

3.1. Apoptosis and β 3-adrenergic stimulation activate Panx1 channels in brown adipocytes

To investigate the role of Panx1 channel function in brown adipocytes, we performed a series of *in vitro* studies using immortalized pre-adipocytes that were differentiated into mature adipocytes [35] (referred to as iBACs hereafter). Panx1 channels are irreversibly activated by caspase-mediated cleavage of the self-inhibitory C-terminal region [23], leading to channel opening and ATP release. We first addressed the question of whether this previously described caspase

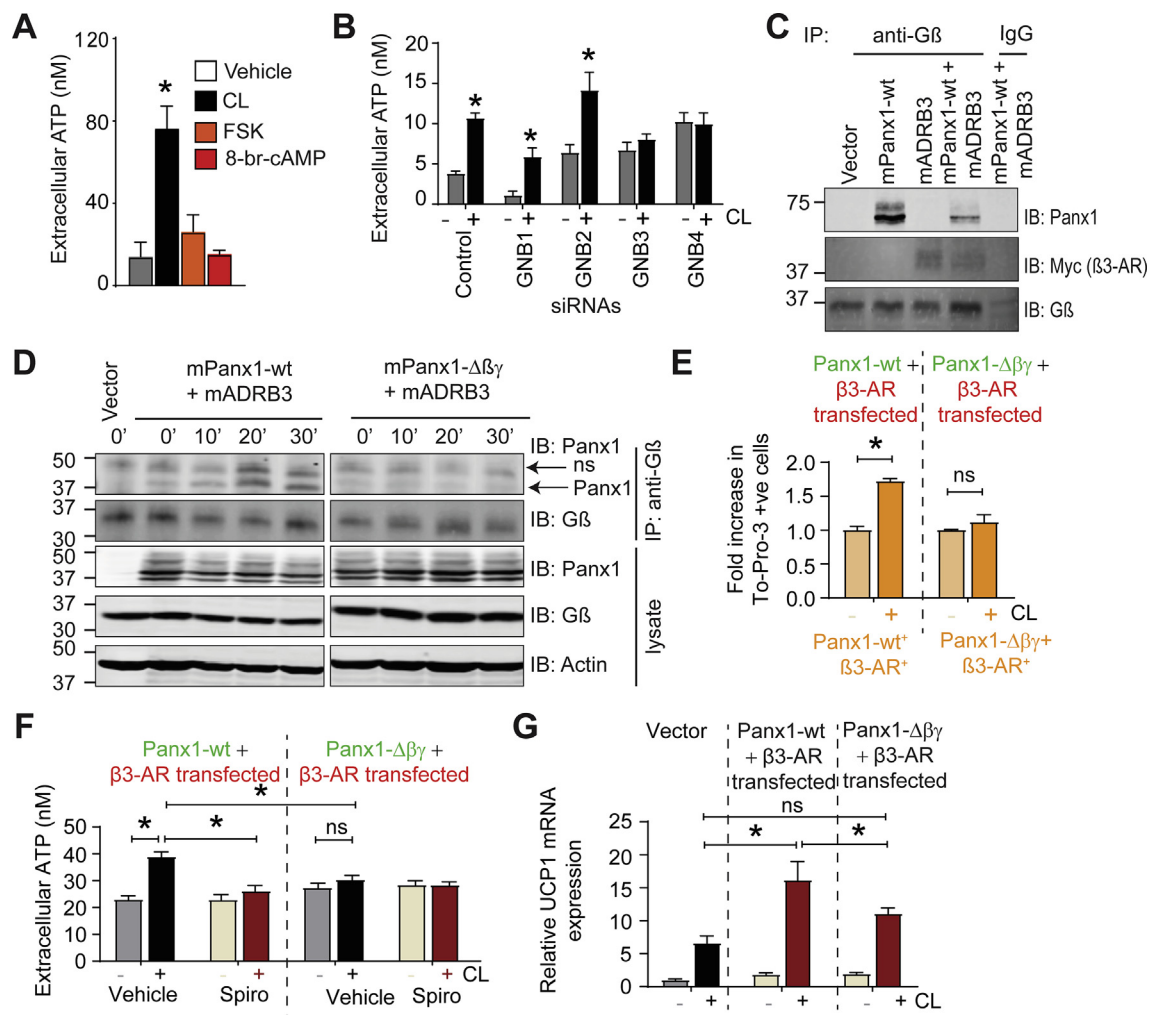


Figure 2: G β γ subunits mediate β 3AR-induced, Panx1-dependent ATP release in brown adipocytes. **A**, ATP release from iBACs treated with 100 nM of CL316243, 50 μ M of forskolin or 10 μ M of 8-Bromo-cAMP for 30 min. **B**, ATP release from iBACs transfected with 50 nM of control siRNA or siRNAs for G β subunits (GNB1-4) for 48 h and then treated with 100 nM of CL316243 for 30 min. **C**, Co-immunoprecipitation of Panx1-G β γ . 293T cells were transfected with plasmids encoding mouse GFP-Panx1 or mouse myc-ADRB3 alone or together. G β subunits were immunoprecipitated and Panx1 in the immunocomplex analyzed by Western blotting. **D**, β 3-agonist induced Panx1-G β γ interaction in 293T cells. Forty-eight hours after transfection with mouse WT-Panx1 or Δ G β γ mutant Panx1 and ADRB3, cells were treated with CL316243 for indicated time points. G β subunits were immunoprecipitated, and Panx1 in the immunocomplex was analyzed by Western blotting. **E**, Flow cytometric analysis of To-Pro-3 uptake in 293T cells transfected with GFP-Panx1-wt or GFP-Panx1 mutant (Panx1- Δ β γ) and mCherry- β 3AR. **F**, ATP release from 293T cells transfected with Panx1-wt or Panx1 mutant (Panx1- Δ β γ) and β 3AR. Forty-eight hours after transfection, cells were treated with 200 nM of CL316243 for 30 min. UCP1 mRNA expression in iBACs transfected with Panx1-wt or Panx1 mutant (Panx1- Δ β γ) and β 3AR. Forty-eight hours after transfection, cells were treated with 100 nM of CL316243 for 6 h. Statistical significance was calculated using one-way ANOVA with Dunnett post-hoc test (A) two-way ANOVA with Tukeys post-hoc test (B, F-G), one-way ANOVA with Dunnett post-hoc test (D), or two-tailed unpaired Student's *t*-test (E). * indicates $p < 0.05$. Error bars, s. e.m.

3-dependent cleavage mechanism can activate Panx1 channels in brown adipocytes as well. Induction of apoptosis in iBACs using UV-light caused opening of Panx1 channels, as demonstrated by characteristic Panx1 currents that were inhibited by carbenoxolone (Figure 1A). UV light exposure induced caspase-3 activity, which was inhibited by *z-vad-fmk* but not by Panx1 inhibitors (Figure S1A). Furthermore, UV light-induced opening of Panx1 channels led to the release of ATP, which was suppressed by pre-treatment of cells with Panx1 inhibitors carbenoxolone, trovafloxacin, or spironolactone, as well as by a pan-caspase inhibitor, *z-vad-fmk* (Figure 1B).

Panx1 channel opening has been described through activation of G α q-coupled receptors. A recent study reported that phenylephrine, a ligand for G α q-coupled α 1-adrenergic receptor activates Panx1 in white adipocytes, at least in part, through a cAMP-PKA pathway probably through

activation of β 2-receptors [34]. However, it is unknown whether Panx1 channels can also be activated in brown adipocytes via stimulation of the β 3AR involving adenylate cycles-cAMP-PKA pathway. We found that treatment of iBACs with the β 3AR agonist CL316243 induced ATP release, which was significantly reduced by Panx1 inhibitors carbenoxolone or spironolactone (Figure 1D), as well as by RNAi-mediated knockdown of Panx1 (Figure 1E, Figure S1B). In addition to releasing small molecules, such as ATP, activated Panx1 channels mediate the entry of specific dyes (Yo-Pro-1, To-Pro-3) into cells (Figure 1C) [22]. Accordingly, treatment with CL316243 induced Yo-Pro-1 dye uptake into iBACs, which was blocked by pretreatment with the Panx1 inhibitors probenecid or spironolactone (Figure 1F). Moreover, Panx1 channel inhibition significantly reduced β 3-agonist-induced lipolysis (Figure S1C), UCP1 expression (Figure S1D), and glucose uptake in iBACs (Figure S1E).

Panx1 appears to function immediately downstream of β 3AR, since inhibition of Panx1 significantly decreased β 3AR-agonist-induced, but not forskolin-induced lipolysis (Figure S1F). To investigate regulation of Panx1 by β 3AR, we used a heterologous expression system consisting of 293T cells transiently transfected with control GFP or GFP-tagged Panx1, together with mCherry-T2A- β 3AR (ADRB3). Treatment with the β 3AR agonist CL316243 induced To-Pro-3 dye uptake in cells that co-expressed Panx1 and ADRB3, but not in cells expressing either GFP-Panx1 or mCherry-ADRB3 alone or in cells co-expressing control GFP and mCherry-ADRB3 (Figure 1G, Figure S2A). Moreover, CL316243 treatment significantly increased ATP release from cells co-expressing Panx1 and ADRB3, which was inhibited by Panx1 inhibitors trovafloxacin and spironolactone (Figure 1H). Together, these results demonstrate that Panx1 channel opening is induced through activation of the β 3AR.

3.2. $G\beta\gamma$ subunits mediate β 3AR-induced, Panx1-dependent ATP release in brown adipocytes

Although CL316243 induced a significant increase in ATP release from iBACS, neither forskolin, a direct activator of adenylate cyclase, nor the cAMP analog 8-bromo-cAMP, induced ATP release from iBACS (Figure 2A), suggesting a $G\alpha s$ -independent mechanism of Panx1 opening. To examine a possible involvement of $G\beta\gamma$ subunits in β 3AR-mediated Panx1 channel activation, we used (i) “ $G\beta\gamma$ sinks” (by transfection of iBACS with plasmids encoding the c-terminal tail region of GRK2 (β ARK-ct) or $G\alpha t$ (transducin) [37], (ii) $G\beta\gamma$ inhibitors gallein [39] or GRK2i [40], and (iii) the $G\beta\gamma$ -activating peptide mSIRK or the inactive peptide mSIRK-L9A [41]. Expression of “ $G\beta\gamma$ sinks” significantly inhibited CL316243-induced ATP release (Figure S3A), as did pretreatment of iBACS with $G\beta\gamma$ inhibitors gallein or GRK2i (Figure S3B). Treatment of iBACS with the $G\beta\gamma$ -activating peptide mSIRK, but not the control peptide, induced a 3-fold increase in ATP release, which was partially inhibited by gallein (Figure S3C). Furthermore, mSIRK-induced ATP release was significantly reduced in iBACS transfected with Panx1 siRNA (Figure S3D). $G\beta\gamma$ released from different GPCRs are reported to have divergent biological effects [42]. To identify the $G\beta$ subunit involved in Panx1 channel activation, we performed siRNA-mediated knockdown of individual $G\beta$ subunits (Figure S2B) and measured β 3AR ligand-induced ATP release in iBACS. CL316243-induced ATP release was abolished in cells transfected with siRNAs for $G\beta$ subunits 3 or $G\beta$ subunits 4 (GNB3 or GNB4), but not $G\beta$ subunits 1 (GNB1) or $G\beta$ subunits 2 (GNB2) (Figure 2B). Taken together, these data provide the first evidence for a role of $G\beta$ subunits in mediating Panx1 channel activation.

Previous studies have shown that $G\beta\gamma$ subunits modulate ion channel activity by directly binding to the channel [43,44]. To investigate whether $G\beta\gamma$ subunits interact with Panx1 channels and if β 3-adrenergic activation modulates this interaction, we performed immunoprecipitation studies using heterologous expression of mouse Panx1 and β 3AR (ADRB3) in 293T cells. Pull-down using an anti- $G\beta$ antibody demonstrated Panx1 and ADRB3 protein–protein interaction (Figure 2C). Primary sequence analysis of Panx1 revealed the presence of a putative $G\beta\gamma$ binding consensus sequence, QXXQ/ER [42] in the C-terminal region of mouse Panx1 (Figure S3E), and we produced mutant Panx1 that lacks this binding site (Panx1- $\Delta\beta\gamma$). While CL316243 treatment induced a time-dependent increase in wild-type Panx1- $G\beta$ interaction in 293T cells, this interaction was abrogated in cells over-expressing mutant Panx1 (Panx1- $\Delta\beta\gamma$) (Figure 2D). Furthermore, in cells over-expressing Panx1- $\Delta\beta\gamma$, CL316243 failed to induce To-pro-3 dye uptake (Figure 2E) and Panx1-dependent ATP-release (Figure 2F). Finally, overexpression of Panx1-wt, but not Panx1-

$\Delta\beta\gamma$, enhanced CL316243-induced induction of UCP1 gene expression (Figure 2G). These data provide evidence for the functional importance of the $G\beta\gamma$ binding site in Panx1, and they demonstrate that $G\beta\gamma$ -dependent Panx1 channel activation plays a critical role in β 3AR-induced thermogenic gene expression in brown adipocytes.

3.3. Panx1 channels regulate thermogenesis in brown adipocytes

Next, we examined the role of Panx1 channels in regulating heat production in brown adipocytes using cellular temperature probes [38,45]. Single-cell thermometry showed that pre-treatment of iBACS with the Panx1 inhibitors carbenoxolone or spironolactone significantly reduced the β 3AR-agonist-induced increase in cellular temperature (Figure 3). These data show that Panx1 channel function is involved in regulation of cellular thermogenesis in brown adipocytes.

3.4. Panx1 deficiency in all adipocytes impacts the thermogenic response in Panx1^{Adip-/-} mice

We have previously produced adipose tissue-specific Panx1 knockout mice (Panx1^{Adip-/-}), which lack Panx1 in all adipose tissue depots [32], including BAT (Figure S4A). However, whether Panx1 controls brown adipocyte function has not been reported. To elucidate a possible functional role of Panx1 in BAT *in vivo*, we performed microPET-imaging in Panx1^{Adip-/-} mice. When housed at 23°C, basal 2-deoxy-2-[fluorine-18]fluoro-D-glucose (¹⁸F-FDG) uptake was slightly higher in BAT of Panx1^{Adip-/-} mice (Table S1). Treatment with a specific β 3AR agonist (CL316243) [46,47] induced a 6-fold increase of ¹⁸F-FDG uptake in BAT of wild-type (Panx1^{fl/fl}) mice, while BAT of Panx1^{Adip-/-} mice was refractory to β 3AR-induced activation (Figure 4A). Treatment

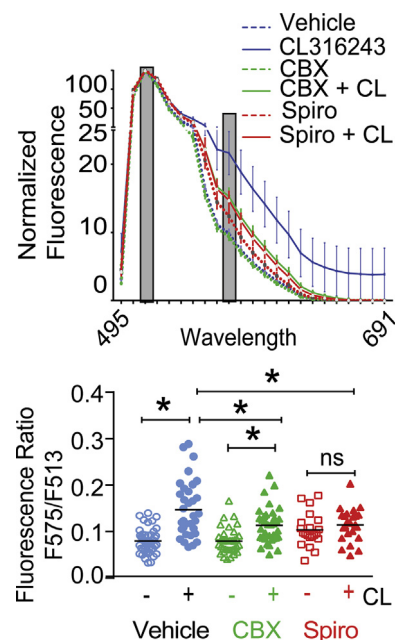


Figure 3: Panx1 channels regulate thermogenesis in brown adipocytes. Temperature measurement using ratiometric fluorescence thermal probes in brown adipocyte. iBACS were pre-treated with Panx1 inhibitors (50 μ M) and then treated with 100 nM CL316243 for 2 h. Normalized fluorescence (top) as well as the fluorescence ratio (F_{575}/F_{513}) (bottom) are shown. Gray bars indicate area that was used for calculation of the ratio. Statistical significance was calculated using two-way ANOVA with Tukey's post-hoc test. * indicates $p < 0.05$. Error bars, s. e.m. Experiments were performed with a minimum of 3 replicates and repeated at least twice. CBX, carbenoxolone; Spiro, spironolactone.

with the β 3AR agonist induced brown adipocyte hypertrophy in wild-type mice without inducing hyperplasia, as has been reported previously [46]. However, brown adipocyte size was unchanged in $Panx1^{Adip-/-}$ mice in response to the β 3AR agonist (Figure 4B, Figure S4B). Thermogenic gene expression was higher in BAT of untreated $Panx1^{Adip-/-}$ mice (Figure S4C), but in response to pharmacological adrenergic activation (Figure 4C) or to cold (4°C) exposure (Figure 4D), induction of thermogenic gene expression was significantly blunted in BAT of $Panx1^{Adip-/-}$ mice compared to $Panx1^{fl/fl}$ mice. Moreover, analysis of cold-induced thermogenesis using telemetric probes implanted in the interscapular region demonstrated that $Panx1^{Adip-/-}$ mice failed to recover normal BAT temperature (Figure 4E). Analyses of overall UCP1 protein levels by Western blotting did not show significant differences between the genotypes after cold exposure (Figure S4D) or pharmacological adrenergic activation (Figure S4E). Exposure to cold led to increased food consumption (Figure S4F), and $Panx1^{Adip-/-}$ mice showed a trend to increased body weight (Figure S4G). Furthermore, cold-induced thermogenic gene expression in scWAT was significantly reduced in $Panx1^{Adip-/-}$ mice (Figure S5A), indicating a defect in beigeing of WAT. Together, these data indicate that $Panx1$ channel function in adipocytes contributes to the regulation of adaptive thermogenesis and to beigeing of subcutaneous adipose tissue.

3.5. $Panx1$ deficiency specifically in brown adipocytes in $Panx1^{BAT-/-}$ mice results in defective cold-induced thermogenesis and exacerbated diet-induced obesity and insulin resistance

To address the physiological importance of $Panx1$ specifically in BAT *in vivo*, we crossed $Panx1^{fl/fl}$ mice with transgenic mice that express Cre recombinase under the control of the UCP-1 promoter, producing brown adipocyte-specific $Panx1$ knockout mice ($Panx1^{BAT-/-}$). UCP1-Cre-mediated $Panx1$ deletion was confirmed in BAT (Figure 5A). Unlike $Panx1^{Adip-/-}$ mice, $Panx1^{BAT-/-}$ mice did not show a difference in thermogenic gene expression at 23°C (Figure S6A). However, upon exposure to cold, $Panx1^{BAT-/-}$ mice exhibited significantly suppressed adaptive thermogenesis (Figure 5B), despite consuming

significantly more food than their respective wild-type littermates (Figure 5C). Similar to $Panx1^{Adip-/-}$ mice, $Panx1^{BAT-/-}$ mice housed at 4°C showed a trend to increased body weight (Figure 5D). Moreover, thermogenic gene expression was significantly reduced in BAT (Figure 5E), but not in scWAT in $Panx1^{BAT-/-}$ mice housed at 4°C (Figure S5B).

Next, we examined whether the suppressed thermogenic capacity of $Panx1^{BAT-/-}$ would result in increased susceptibility to obesity or insulin resistance. We found that $Panx1^{BAT-/-}$ mice fed a diabetogenic diet (60% fat) gained significantly more weight (Figure 5F, Figure S6B) than their wild type littermates. Consistent with increased body weight, $Panx1^{BAT-/-}$ exhibited increased fat mass without any alteration in lean mass (Figure 5G, Figure S6C, Figure S6D), despite consuming the same amount of food as their littermates (Fig 5H). Finally, the absence of $Panx1$ in brown adipocytes rendered $Panx1^{BAT-/-}$ mice more susceptible to diet-induced insulin resistance (Figure 5I, J).

4. DISCUSSION

Functional studies in rodents and the identification of BAT in adult humans [48–50] have highlighted the potential benefits of brown adipose-targeted therapeutic approaches for obesity and associated metabolic complications [51,52]. Moreover, abnormal activation of BAT has been suggested to play a role in some forms of cancer cachexia [53–55]. Although β 3-adrenergic receptor agonists have been shown to activate BAT in humans [56–58], the enthusiasm for their use in clinics is dampened due to associated cardiovascular risks. Therefore, a better understanding of mechanisms involved in brown adipocyte activation is essential for the development of novel therapeutic strategies. Our study identifies $Panx1$ channels to be involved in regulating β 3-adrenergic-receptor-induced thermogenesis in brown adipocytes and whole-body energy metabolism in mice.

We found that $Panx1$ channel inhibition in an immortalized brown adipocyte line (iBAC) significantly reduced β 3-agonist-induced lipolysis, glucose uptake, and thermogenic gene expression. Since fatty

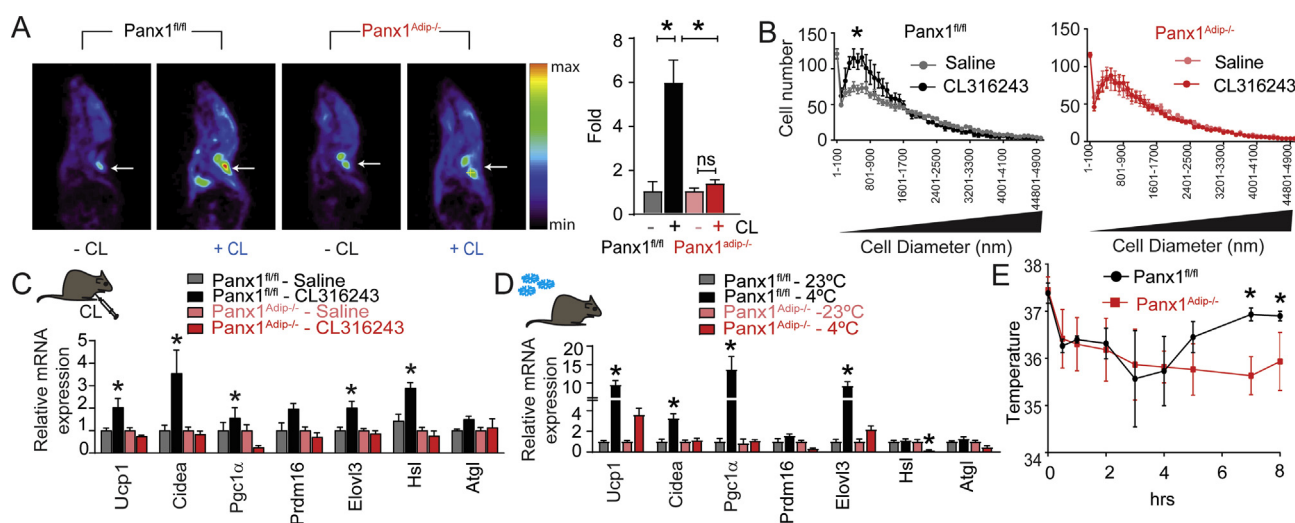


Figure 4: Defective brown adipose tissue (BAT) function in $Panx1^{Adip-/-}$ mice. **A**, Positron emission tomography of ^{18}F -FDG uptake into brown adipose tissue of $Panx1^{fl/fl}$ or $Panx1^{Adip-/-}$ mice treated with saline or CL316243 (1 mg/kg b. wt. i. p) for 24 h ($n = 4$). **B**, Frequency distribution of adipocyte size in BAT from $Panx1^{fl/fl}$ or $Panx1^{Adip-/-}$ mice treated with saline or CL316243 (1 mg/kg b. wt. i. p) for 6 d ($n = 3-5$). **C**, Thermogenic gene expression in the BAT of $Panx1^{fl/fl}$ or $Panx1^{Adip-/-}$ mice treated with saline or CL316243 (1 mg/kg b. wt. i. p) for 6 d ($n = 6-8$). **D**, Thermogenic gene expression in BAT of cold-exposed $Panx1^{fl/fl}$ or $Panx1^{Adip-/-}$ mice compared to mice housed at 23°C ($n = 5-9$). **E**, BAT temperature in $Panx1^{fl/fl}$ and $Panx1^{Adip-/-}$ mice exposed to cold (4°C) ($n = 3$). Statistical significance was calculated using two-way ANOVA with Tukey's post-hoc test (A–D) or two-tailed unpaired Student's *t*-test (E). * indicates $p < 0.05$. Error bars, s. e. m.

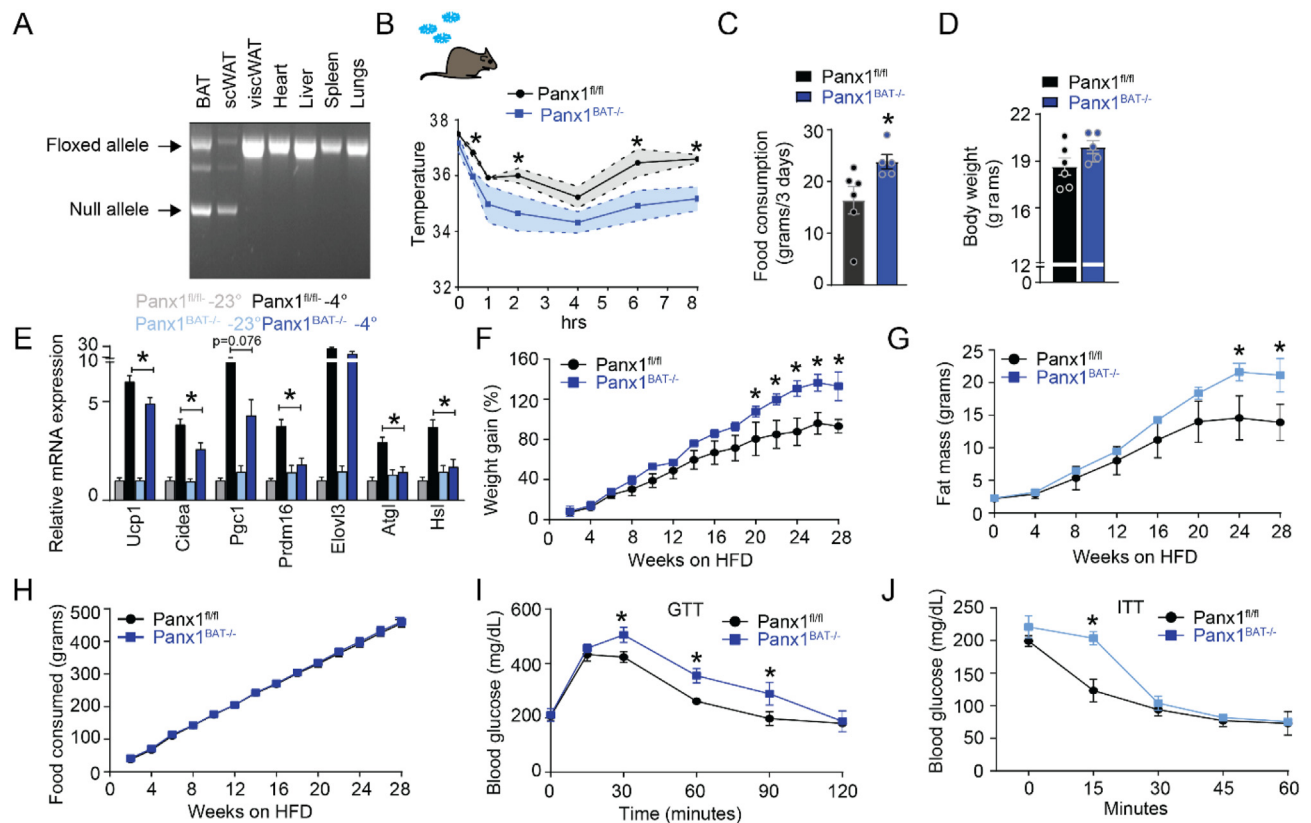


Figure 5: $Panx1^{BAT-/-}$ mice exhibit defective cold-induced thermogenesis and exacerbated diet-induced obesity and insulin resistance. **A**, PCR analysis of $Panx1$ deletion in different tissues of $Panx1^{BAT-/-}$ mice. **B**, BAT temperature in $Panx1^{fl/fl}$ and $Panx1^{BAT-/-}$ mice exposed to cold (4°C) ($n = 3$). **C**, Food consumption by $Panx1^{fl/fl}$ and $Panx1^{BAT-/-}$ mice at 4°C ($n = 6$). **D**, Body weight of $Panx1^{fl/fl}$ and $Panx1^{BAT-/-}$ mice at 4°C ($n = 6$). **E**, Expression of genes involved in thermogenesis in $Panx1^{fl/fl}$ and $Panx1^{BAT-/-}$ mice at 4°C . **F**, Weight gain. **G**, fat mass. **H**, food consumption, **I**, glucose tolerance, and **J**, insulin tolerance in $Panx1^{fl/fl}$ and $Panx1^{BAT-/-}$ mice fed high-fat diet for 28 weeks ($n = 4$). Statistical significance was calculated using two-tailed unpaired Student's *t*-test (B–D), two-way ANOVA with Tukeys post-hoc test (E) or two-way ANOVA with Fisher's LSD test (F–J). * indicates $p < 0.05$. Error bars, s. e. m.

acids and glucose are two major substrates utilized by activated brown adipocytes, these data suggest that $Panx1$ regulates brown adipocyte function, at least in part, by suppressing substrate availability and utilization. Currently, the mechanism by which $Panx1$ channel activity regulates brown adipocyte function is unknown. The effects we observed seem to be independent of the release of nucleotides or nucleosides via open $Panx1$ channels and subsequent autocrine purinergic signaling, since neither addition of exogenous ATP or adenosine, nor pharmacologic inhibition of purinergic receptors rescued the effect of $Panx1$ channel inhibition (data not shown). However, we cannot exclude the possibility that $\beta 3\text{AR}$ -induced $Panx1$ channel opening controls intracellular ATP levels, and/or mediates the release of yet to be identified metabolites [59] that may constitute a feed forward signaling to sustain $\beta 3$ -adrenergic signaling. Among such metabolites, succinate within brown adipose tissue has been reported to modulate cold-induced thermogenesis in mice [60]. However, in this study succinate accumulation was cold-specific and was not observed upon acute $\beta 3$ -agonist treatment, while in our study $Panx1$ knockdown suppressed both cold-induced and $\beta 3$ -agonist-induced brown fat function. Nevertheless, the role of $Panx1$ -dependent release of metabolites in thermogenic regulation requires further investigation.

We demonstrate that $\beta 3$ -adrenergic stimulation induces $Panx1$ channel activation, which involves the $G\beta\gamma$ subunits of this $G\alpha s$ -coupled GPCR. Whether this mechanism is specific for brown

adipocytes remains to be shown; nevertheless, we observed differences in the response to beta adrenergic-dependent $Panx1$ channel activation between brown and white adipocytes. While a recent study in white adipocytes has shown activation of $Panx1$ by cAMP analogs, adenylate cyclase activators, and phenylephrine by a cAMP-PKA-dependent pathway [34], we found $\beta 3\text{AR}$ -dependent $Panx1$ channel activation in iBACs to be independent of the adenylate-cyclase-cAMP pathway and rather to involve $G\beta\gamma$ subunits. In our earlier report, we showed that suppressed white adipocyte function in $Panx1$ inhibitor-treated cells can be rescued with exogenous addition of ATP [32], while in the current study, we found that suppressed brown adipocyte function in $Panx1$ inhibitor-treated cells could not be rescued by exogenous purine nucleotides. Differences in response to purinergic activation, in expression levels of isoforms of α and β receptors, or in cellular metabolic status could all account for different responses of white and brown adipocytes.

We also demonstrate the patho-physiological importance of $Panx1$ function in thermogenesis and whole-body energy metabolism using tissue-specific $Panx1$ knockout mice that are deficient for $Panx1$ either in all adipose depots ($Panx1^{Adip-/-}$) or only in brown adipocytes ($Panx1^{BAT-/-}$). In either mouse model, $Panx1$ deficiency led to a defective thermogenic response, illustrated by a reduced expression of thermogenic genes. Although $Panx1$ knockout mice exhibited reduced UCP1 mRNA expression after cold exposure or CL316243 treatment, Western blotting revealed no significant difference of UCP1 protein

content in BAT. Further investigation is needed to determine the reason for this disconnect, but it may be a result of additional regulatory mechanisms, such as an increase in UCP1 mRNA translation [61] or post-translational stabilization of UCP1 protein [62], to compensate for decreased gene transcription.

Interestingly, the effect of Panx1 knockdown was more profound *in vivo* than the observed *in vitro* effect on lipolysis. It should be noted that recent studies have demonstrated lipolysis-independent regulation of thermogenesis in brown adipocytes [15]. In these studies, BAT-specific knockdown of lipolytic enzymes did not have any profound effect on thermogenesis. Since we show that Panx1 inhibition also affects other cellular functions, including glucose uptake, it is possible that the cumulative effect of Panx1 on individual processes leads to the profound effect seen *in vivo*.

Recent studies have reported the presence of Panx1 in preadipocytes and global deletion of Panx1 was shown to promote adipogenesis leading to elevated fat mass in Panx1 null mice without any obvious difference in weight gain [33]. However, in mice with adipose-specific Panx1 knockdown, the expression levels of adipogenic markers, such as FABP4 and PPAR γ , were not significantly altered in brown or subcutaneous white adipose tissue (data not shown), indicating that the observed differences in thermogenic potential are independent of adipocyte differentiation.

We observed that cold-induced browning (beigeing) of WAT was attenuated in Panx1^{Adip^{-/-}} mice, but not in Panx1^{BAT^{-/-}} mice. We speculate that the underlying mechanism for the observed difference between the genotypes lies in the temporal difference of Panx1 expression in mature white adipocytes and preadipocytes. Since beigeing of white adipose tissue occurs either through transdifferentiation of existing white adipocytes or via recruitment of new beige adipocytes from existing preadipocytes, we speculate that both processes could be affected in Panx1^{Adip^{-/-}} mice, in which Cre expression is under the control of the adiponectin promoter, which would effectively delete Panx1 in both cell types. On the other hand, in Panx1^{BAT^{-/-}} mice, in which Cre expression is under the control of the UCP promoter, the majority of the white adipocytes or preadipocytes still express Panx1, and Panx1 deletion occurs only at the instance of active UCP1 transcription, which then would not be sufficient to inhibit browning of white adipose tissue. In any case, the effect of Panx1 on WAT browning is in itself an interesting phenomenon that requires further investigation.

In mice that were deficient for Panx1 in all adipose depots (Panx1^{Adip^{-/-}} mice), we observed compensatory activation of BAT at the basal state. We speculate that this could be due to the impaired cold adaptation of WAT in Panx1^{Adip^{-/-}} mice, since the thermoneutral temperature for mice is 29–30°C, and when housed at 23°C, mice are considered to be under mild cold-stress. Compensatory BAT activation at mild cold (23°C) was not observed in Panx1^{BAT^{-/-}} mice, which lack Panx1 specifically in brown adipocytes, and thus it is plausible that the compensatory increase in BAT thermogenesis in Panx1^{Adip^{-/-}} mice under mild cold exposure could be due to reduced WAT beigeing as seen in Panx1^{Adip^{-/-}} mice, but not in Panx1^{BAT^{-/-}}.

Finally, we show that Panx1 deletion specifically in brown adipocytes (Panx1^{BAT^{-/-}} mice) aggravated diet-induced obesity and insulin resistance, consistent with reduced energy expenditure and impaired control of diet-induced thermogenesis. Previously, aggravated diet-induced insulin resistance in the absence of significant differences in weight gain has been reported in Panx1^{Adip^{-/-}} mice [32], while increased fat mass was observed in global Panx1^{-/-} mice [33]. Differences in experimental conditions may have determined the outcome of these studies. While female mice were used in the current study, in the previous studies male mice were used. Moreover, the duration for

which the mice were kept on a high-energy diet was different. While the two earlier studies involved feeding for a duration of 12–15 weeks, the current study involved feeding for an extended period of 30 weeks. The data from the current study reveal that significant differences in weight gain occurred only after 20 weeks on the diet. Therefore, further studies are required to elucidate the exact role of adipocyte Panx1 in overall weight gain.

Together, our data identify Panx1 channels as key regulators of β -adrenergic-induced brown adipocyte activation, and we demonstrate that the absence of Panx1 significantly impacts β -adrenergic receptor-induced adaptive thermogenesis in brown adipocytes and in mice. Targeting Panx1 could be a therapeutic strategy to treat a variety of conditions with aberrant BAT function [63,64].

FUNDING

This study was supported by NIH, USA P01 grant HL120840 (to NL, BND, UML); NIH, USA R01 grant HL 123627 (to BKK); Development of Advanced Measurement and Analysis System by JST, Japan (to SU and NI); Grant-in-Aid for Scientific Research for Plant Graduate Students from Nara Institute of Science and Technology by MEXT, Japan (to NI); The Mitsubishi Foundation, Japan (ID:25103, to NI), and Grant-in-Aid for Scientific Research, Japan (17H03075, to SU). VS was supported by pre-doctoral fellowships from the NIH, USA (5 F31 DK108553-02), AHA, USA (15 PRE 255600036), and Pharmacological Sciences Training Grant, NIH, USA (5 T32 GM007055-40).

AUTHOR CONTRIBUTIONS

NL conceived the project, designed experiments, and wrote the manuscript; SS conceived the project, designed and conducted experiments, analyzed data, and wrote the manuscript; VS and CU conducted experiments and analyzed data. SKM and BND performed patch-clamp analysis of Panx1 currents and analyzed data; SS performed genotyping analysis, co-immunoprecipitation, and immunoblotting; AKM performed single-cell thermometry experiments and analyzed data; UML managed Panx1 mouse core and provided mice used in the study; TEH provided expertise and guidance on adipocyte culture and transfection, and on lipolysis and adrenergic signaling experiments; KWA and SRK performed metabolic cage experiments and analyzed data; MC and BKK performed PET imaging and analyzed data; PJ and AK performed flow cytometry and analyzed data; LS performed morphometric analysis of brown adipocytes; RP-G quantified UCP immunostaining; NO performed the glucose uptake studies; SU and NI provided the ratiometric fluorescent thermometer.

ACKNOWLEDGMENTS

We thank Dr. Bruce Spiegelman (Department of Cell Biology, Harvard Medical School, USA) for providing the immortalized brown-preadipocyte cell line and Dr. Douglas A. Bayliss (Department of Pharmacology, University of Virginia, USA) for sharing the $\beta\gamma$ -sinks. We acknowledge the use of the following core facilities: pannexin mouse and physiology cores, histology core at the Robert M. Berne Cardiovascular Research Center, University of Virginia Molecular Imaging Core and University of Virginia Flow Cytometry Core.

APPENDIX A. SUPPLEMENTARY DATA

Supplementary data to this article can be found online at <https://doi.org/10.1016/j.molmet.2020.101130>.

CONFLICT OF INTEREST

Authors declare no competing interests.

REFERENCES

- [1] Rothwell, N.J., Stock, M.J., 1979. A role for brown adipose tissue in diet-induced thermogenesis. *Nature* 281:31–35.
- [2] Klingenspor, M., 2003. Cold-induced recruitment of brown adipose tissue thermogenesis. *Experimental Physiology* 88:141–148.
- [3] Cannon, B., Nedergaard, J., 2004. Brown adipose tissue: function and physiological significance. *Physiological Reviews* 84:277–359.
- [4] Razzoli, M., Emmett, M.J., Lazar, M.A., Bartolomucci, A., 2018. beta-Adrenergic receptors control brown adipose UCP-1 tone and cold response without affecting its circadian rhythmicity. *The FASEB Journal : Official Publication of the Federation of American Societies for Experimental Biology* 32:5640–5646.
- [5] Lee, P., Swarbrick, M.M., Ho, K.K., 2013. Brown adipose tissue in adult humans: a metabolic renaissance. *Endocrine Reviews* 34:413–438.
- [6] Bronnikov, G., Bengtsson, T., Kramarova, L., Golozubova, V., Cannon, B., Nedergaard, J., 1999. beta1 to beta3 switch in control of cyclic adenosine monophosphate during brown adipocyte development explains distinct beta-adrenoceptor subtype mediation of proliferation and differentiation. *Endocrinology* 140:4185–4197.
- [7] Cannon, B., Nedergaard, J., 2017. What ignites UCP1? *Cell Metabolism* 26: 697–698.
- [8] Cohen, P., Spiegelman, B.M., 2015. Brown and beige fat: molecular parts of a thermogenic machine. *Diabetes* 64:2346–2351.
- [9] Shabalina, I.G., Backlund, E.C., Bar-Tana, J., Cannon, B., Nedergaard, J., 2008. Within brown-fat cells, UCP1-mediated fatty acid-induced uncoupling is independent of fatty acid metabolism. *Biochimica et Biophysica Acta* 1777: 642–650.
- [10] Matthias, A., Ohlson, K.B., Fredriksson, J.M., Jacobsson, A., Nedergaard, J., Cannon, B., 2000. Thermogenic responses in brown fat cells are fully UCP1-dependent. UCP2 or UCP3 do not substitute for UCP1 in adrenergically or fatty acid-induced thermogenesis. *Journal of Biological Chemistry* 275:25073–25081.
- [11] Klingenberg, M., 2017. UCP1 - a sophisticated energy valve. *Biochimie* 134: 19–27.
- [12] Bouillaud, F., Alves-Guerra, M.C., Ricquier, D., 2016. UCPs, at the interface between bioenergetics and metabolism. *Biochimica et Biophysica Acta* 1863: 2443–2456.
- [13] Lee, Y., Willers, C., Kunji, E.R., Crichton, P.G., 2015. Uncoupling protein 1 binds one nucleotide per monomer and is stabilized by tightly bound cardiolipin. *Proceedings of the National Academy of Sciences of the United States of America* 112:6973–6978.
- [14] Swida-Barteczka, A., Woyda-Ploszczycza, A., Sluse, F.E., Jarmuszkiewicz, W., 2009. Uncoupling protein 1 inhibition by purine nucleotides is under the control of the endogenous ubiquinone redox state. *Biochemical Journal* 424:297–306.
- [15] Schreiber, R., Diwoky, C., Schoiswohl, G., Feiler, U., Wongsiriroj, N., Abdellatif, M., et al., 2017. Cold-induced thermogenesis depends on ATGL-mediated lipolysis in cardiac muscle, but not Brown adipose tissue. *e757 Cell Metabolism* 26:753–763.
- [16] Bal, N.C., Singh, S., Reis, F.C.G., Maurya, S.K., Pani, S., Rowland, L.A., et al., 2017. Both brown adipose tissue and skeletal muscle thermogenesis processes are activated during mild to severe cold adaptation in mice. *Journal of Biological Chemistry* 292:16616–16625.
- [17] Penuela, S., Gehi, R., Laird, D.W., 2013. The biochemistry and function of pannexin channels. *Biochimica et Biophysica Acta* 1828:15–22.
- [18] Chiu, Y.H., Jin, X., Medina, C.B., Leonhardt, S.A., Kiessling, V., Bennett, B., et al., 2017. A quantized mechanism for activation of pannexin channels. *Nature Communications* 8:14324.
- [19] Chiu, Y.H., Schappe, M.S., Desai, B.N., Bayliss, D.A., 2017. Revisiting multimodal activation and channel properties of Pannexin 1. *The Journal of General Physiology*.
- [20] Billaud, M., Chiu, Y.H., Lohman, A.W., Parpaite, T., Butcher, J.T., Mutchler, S.M., et al., 2015. A molecular signature in the pannexin1 intracellular loop confers channel activation by the alpha1 adrenoceptor in smooth muscle cells. *Science Signaling* 8:ra17.
- [21] Chiu, Y.H., Ravichandran, K.S., Bayliss, D.A., 2014. Intrinsic properties and regulation of Pannexin 1 channel. *Channels* 8:103–109.
- [22] Chekeni, F.B., Elliott, M.R., Sandilos, J.K., Walk, S.F., Kinchen, J.M., Lazarowski, E.R., et al., 2010. Pannexin 1 channels mediate 'find-me' signal release and membrane permeability during apoptosis. *Nature* 467:863–867.
- [23] Sandilos, J.K., Chiu, Y.H., Chekeni, F.B., Armstrong, A.J., Walk, S.F., Ravichandran, K.S., et al., 2012. Pannexin 1, an ATP release channel, is activated by caspase cleavage of its pore-associated C-terminal autoinhibitory region. *Journal of Biological Chemistry* 287:11303–11311.
- [24] Ruan, Z., Orozco, I.J., Du, J., Lu, W., 2020. Structures of human pannexin 1 reveal ion pathways and mechanism of gating. *Nature* 584:646–651.
- [25] Penuela, S., Lohman, A.W., Lai, W., Gyenis, L., Litchfield, D.W., Isakson, B.E., et al., 2014. Diverse post-translational modifications of the pannexin family of channel-forming proteins. *Channels* 8:124–130.
- [26] DeLalio, L.J., Billaud, M., Ruddiman, C.A., Johnstone, S.R., Butcher, J.T., Wolpe, A.G., et al., 2019. Constitutive SRC-mediated phosphorylation of pannexin 1 at tyrosine 198 occurs at the plasma membrane. *Journal of Biological Chemistry* 294:6940–6956.
- [27] Lohman, A.W., Weaver, J.L., Billaud, M., Sandilos, J.K., Griffiths, R., Straub, A.C., et al., 2012. S-nitrosylation inhibits pannexin 1 channel function. *Journal of Biological Chemistry* 287:39602–39612.
- [28] Dahl, G., Qiu, F., Wang, J., 2013. The bizarre pharmacology of the ATP release channel pannexin1. *Neuropharmacology* 75:583–593.
- [29] Wang, J., Jackson, D.G., Dahl, G., 2013. The food dye FD&C Blue No. 1 is a selective inhibitor of the ATP release channel Panx1. *The Journal of General Physiology* 141:649–656.
- [30] Good, M.E., Chiu, Y.H., Poon, I.K.H., Medina, C.B., Butcher, J.T., Mendu, S.K., et al., 2017. Pannexin 1 channels as an unexpected new target of the anti-hypertensive drug spironolactone. *Circulation research*.
- [31] Poon, I.K., Chiu, Y.H., Armstrong, A.J., Kinchen, J.M., Juncadella, I.J., Bayliss, D.A., et al., 2014. Unexpected link between an antibiotic, pannexin channels and apoptosis. *Nature* 507:329–334.
- [32] Adamson, S.E., Meher, A.K., Chiu, Y.H., Sandilos, J.K., Oberholtzer, N.P., Walker, N.N., et al., 2015. Pannexin 1 is required for full activation of insulin-stimulated glucose uptake in adipocytes. *Molecular metabolism* 4:610–618.
- [33] Lee, V.R., Barr, K.J., Kelly, J.J., Johnston, D., Brown, C.F.C., Robb, K.P., et al., 2018. Pannexin 1 regulates adipose stromal cell differentiation and fat accumulation. *Scientific Reports* 8:16166.
- [34] Tozzi, M., Hansen, J.B., Novak, I., 2020. Pannexin-1 mediated ATP release in adipocytes is sensitive to glucose and insulin and modulates lipolysis and macrophage migration. *Acta Physiologica* 228:e13360.
- [35] Cooper, M.P., Uldry, M., Kajimura, S., Arany, Z., Spiegelman, B.M., 2008. Modulation of PGC-1 coactivator pathways in brown fat differentiation through LRP130. *Journal of Biological Chemistry* 283:31960–31967.
- [36] Penuela, S., Bhalla, R., Gong, X.Q., Cowan, K.N., Celetti, S.J., Cowan, B.J., et al., 2007. Pannexin 1 and pannexin 3 are glycoproteins that exhibit many distinct characteristics from the connexin family of gap junction proteins. *Journal of Cell Science* 120:3772–3783.
- [37] Lei, Q., Talley, E.M., Bayliss, D.A., 2001. Receptor-mediated inhibition of G protein-coupled inwardly rectifying potassium channels involves G(alpha)q family subunits, phospholipase C, and a readily diffusible messenger. *Journal of Biological Chemistry* 276:16720–16730.

- [38] Uchiyama, S., Tsuji, T., Ikado, K., Yoshida, A., Kawamoto, K., Hayashi, T., et al., 2015. A cationic fluorescent polymeric thermometer for the ratiometric sensing of intracellular temperature. *The Analyst* 140:4498–4506.
- [39] Lehmann, D.M., Seneviratne, A.M., Smrcka, A.V., 2008. Small molecule disruption of G protein beta gamma subunit signaling inhibits neutrophil chemotaxis and inflammation. *Molecular Pharmacology* 73:410–418.
- [40] Koch, W.J., Hawes, B.E., Inglese, J., Luttrell, L.M., Lefkowitz, R.J., 1994. Cellular expression of the carboxyl terminus of a G protein-coupled receptor kinase attenuates G beta gamma-mediated signaling. *Journal of Biological Chemistry* 269:6193–6197.
- [41] Goubaeva, F., Ghosh, M., Malik, S., Yang, J., Hinkle, P.M., Griendling, K.K., et al., 2003. Stimulation of cellular signaling and G protein subunit dissociation by G protein betagamma subunit-binding peptides. *Journal of Biological Chemistry* 278:19634–19641.
- [42] Khan, S.M., Sleno, R., Gora, S., Zylbergold, P., Laverdure, J.P., Labbé, J.C., et al., 2013. The expanding roles of Gbetagamma subunits in G protein-coupled receptor signaling and drug action. *Pharmacological Reviews* 65:545–577.
- [43] Lei, Q., Jones, M.B., Talley, E.M., Garrison, J.C., Bayliss, D.A., et al., 2000. Activation and inhibition of G protein-coupled inwardly rectifying potassium (Kir3) channels by G protein beta gamma subunits. *Proceedings of the National Academy of Sciences of the United States of America* 97:9771–9776.
- [44] Wolfe, J.T., Wang, H., Howard, J., Garrison, J.C., Barrett, P.Q., 2003. T-type calcium channel regulation by specific G-protein betagamma subunits. *Nature* 424:209–213.
- [45] Kimura, H., Nagoshi, T., Yoshii, A., Kashiwagi, Y., Tanaka, Y., Ito, K., et al., 2017. The thermogenic actions of natriuretic peptide in brown adipocytes: the direct measurement of the intracellular temperature using a fluorescent thermoprobe. *Scientific Reports* 7:12978.
- [46] Himms-Hagen, J., Cui, J., Danforth Jr, E., Taatjes, D.J., Lang, S.S., Waters, B.L., et al., 1994. Effect of CL-316,243, a thermogenic beta 3-agonist, on energy balance and brown and white adipose tissues in rats. *American Journal of Physiology* 266:R1371–R1382.
- [47] Bloom, J.D., Dutia, M.D., Johnson, B.D., Wissner, A., Burns, M.G., Largis, E.E., et al., 1992. Disodium (R,R)-5-[2-[[2-(3-chlorophenyl)-2-hydroxyethyl]-amino]propyl]-1,3-benzodioxole-2,2-dicarboxylate (CL 316,243). A potent beta-adrenergic agonist virtually specific for beta 3 receptors. A promising anti-diabetic and antiobesity agent. *Journal of Medicinal Chemistry* 35:3081–3084.
- [48] Cannon, B., Nedergaard, J., 2012. Yes, even human brown fat is on fire! *Journal of Clinical Investigation* 122:486–489.
- [49] Zingaretti, M.C., Crosta, F., Vitali, A., Guerrieri, M., Frontini, A., Cannon, B., et al., 2009. The presence of UCP1 demonstrates that metabolically active adipose tissue in the neck of adult humans truly represents brown adipose tissue. *The FASEB Journal : Official Publication of the Federation of American Societies for Experimental Biology* 23:3113–3120.
- [50] Nedergaard, J., Bengtsson, T., Cannon, B., 2007. Unexpected evidence for active brown adipose tissue in adult humans. *American Journal of Physiology - Endocrinology And Metabolism* 293:E444–E452.
- [51] Betz, M.J., Enerback, S., 2011. Therapeutic prospects of metabolically active brown adipose tissue in humans. *Frontiers in Endocrinology* 2:86.
- [52] Abdullahi, A., Jeschke, M.G., 2017. Taming the flames: targeting white adipose tissue browning in hypermetabolic conditions. *Endocrine Reviews* 38: 538–549.
- [53] Petruzzelli, M., Schweiger, M., Schreiber, R., Campos-Olivas, R., Tsoli, M., Allen, J., et al., 2014. A switch from white to brown fat increases energy expenditure in cancer-associated cachexia. *Cell Metabolism* 20:433–447.
- [54] Beijer, E., Schoenmakers, J., Vijgen, G., Kessels, F., Dingemans, A.M., Schrauwen, P., et al., 2012. A role of active brown adipose tissue in cancer cachexia? *Oncology reviews* 6:e11.
- [55] Shellock, F.G., Riedinger, M.S., Fishbein, M.C., 1986. Brown adipose tissue in cancer patients: possible cause of cancer-induced cachexia. *Journal of Cancer Research and Clinical Oncology* 111:82–85.
- [56] Cypess, A.M., Weiner, L.S., Roberts-Toler, C., Franquet Elia, E., Kessler, S.H., Kahn, P.A., et al., 2015. Activation of human brown adipose tissue by a beta3-adrenergic receptor agonist. *Cell Metabolism* 21:33–38.
- [57] Sui, W., Li, H., Yang, Y., Jing, X., Xue, F., Cheng, J., et al., 2019. Bladder drug mirabegron exacerbates atherosclerosis through activation of brown fat-mediated lipolysis. *Proceedings of the National Academy of Sciences of the United States of America* 116:10937–10942.
- [58] O'Mara, A.E., Johnson, J.W., Linderman, J.D., Brychta, R.J., McGehee, S., Fletcher, L.A., et al., 2020. Chronic mirabegron treatment increases human brown fat, HDL cholesterol, and insulin sensitivity. *Journal of Clinical Investigation* 130:2209–2219.
- [59] Medina, C.B., Mehrotra, P., Arandjelovic, S., Perry, J.S.A., Guo, Y., Morioka, S., et al., 2020. Metabolites released from apoptotic cells act as tissue messengers. *Nature* 580:130–135.
- [60] Mills, E.L., Pierce, K.A., Jedrychowski, M.P., Garrity, R., Winther, S., Vidoni, S., et al., 2018. Accumulation of succinate controls activation of adipose tissue thermogenesis. *Nature* 560:102–106.
- [61] Dai, N., Zhao, L., Wrighting, D., Krämer, D., Majithia, A., Wang, Y., et al., 2015. IGF2BP2/IMP2-Deficient mice resist obesity through enhanced translation of Ucp1 mRNA and Other mRNAs encoding mitochondrial proteins. *Cell Metabolism* 21:609–621.
- [62] Wang, G., Meyer, J.G., Cai, W., Softic, S., Li, E., Verdin, E., et al., 2019. Regulation of UCP1 and mitochondrial metabolism in Brown adipose tissue by reversible succinylation. *e847 Molecular Cell* 74:844–857.
- [63] Sun, X., Feng, X., Wu, X., Lu, Y., Chen, K., Ye, Y., 2020. Fat wasting is damaging: role of adipose tissue in cancer-associated cachexia. *Front Cell Dev Biol* 8:33.
- [64] Chen, K.Y., Brychta, R.J., Abdul Sater, Z., Cassimatis, T.M., Cero, C., Fletcher, L.A., et al., 2020. Opportunities and challenges in the therapeutic activation of human energy expenditure and thermogenesis to manage obesity. *Journal of Biological Chemistry* 295:1926–1942.